

FR

MSUCL 919

Sw 3408



Michigan State University

National Superconducting Cyclotron Laboratory

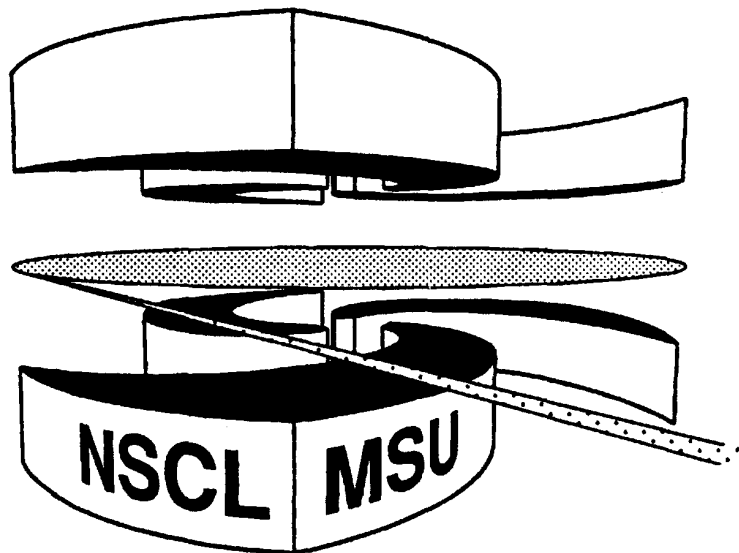
CERN LIBRARIES, GENEVA



P00021220

**NONSTATISTICAL POPULATIONS OF PARTICLE-UNBOUND
STATES IN ^{10}B**

**C. SCHWARZ, W.G. GONG, N. CARLIN, C.K. GELBKE, Y.D. KIM,
W.G. LYNCH, T. MURAKAMI, G. POGGI, R.T. de SOUZA,
M.B. TSANG, H.M. XU, K. KWIATKOWSKI, V.E. VIOLA, and
S. YENNELLO**



MSUCL-919

JANUARY 1994

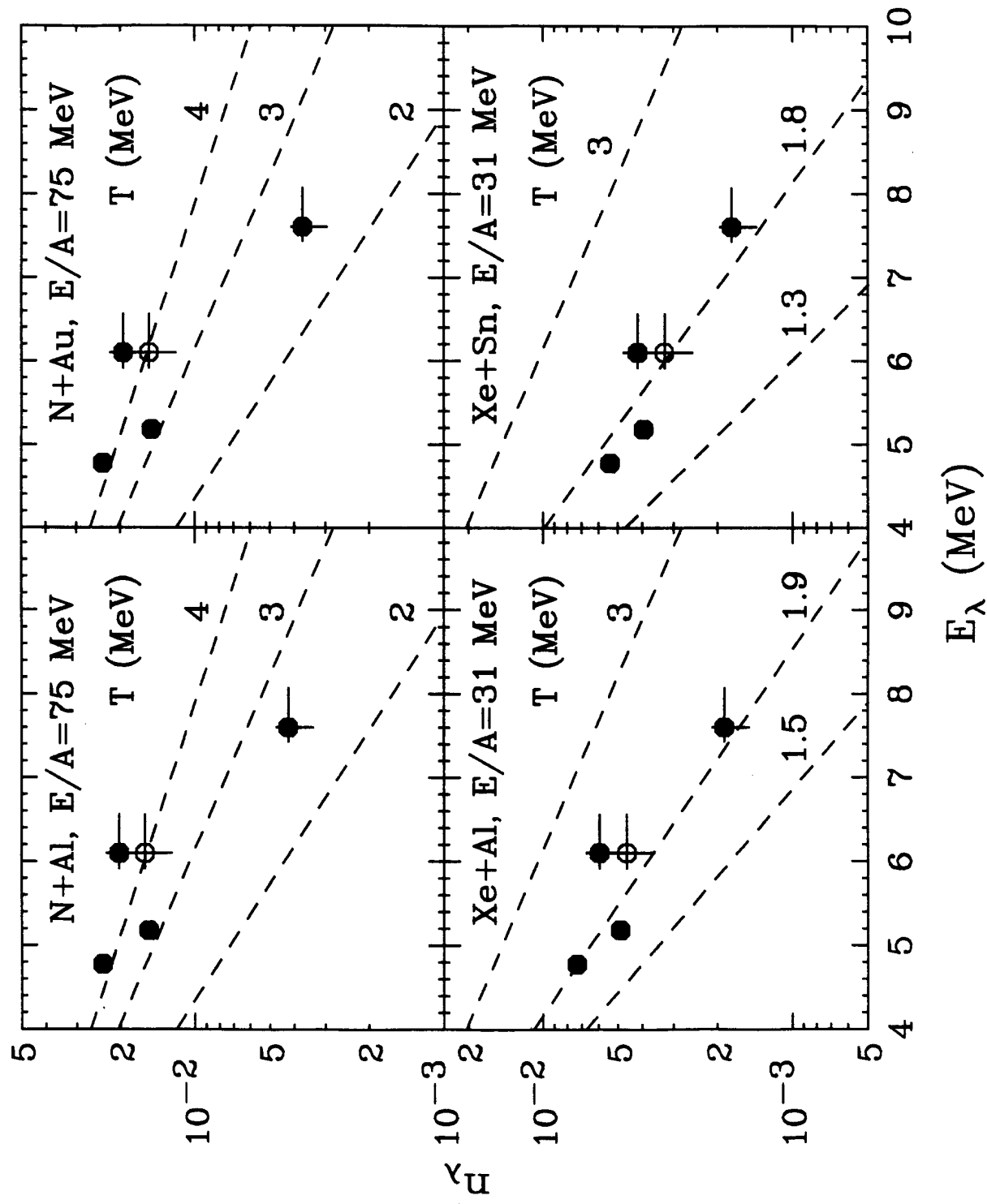


Fig. 4

Nonstatistical Populations of Particle-Unbound States in ^{10}B

C. Schwarz, W.G. Gong^a, N. Carlin^b, C.K. Gelbke, Y.D. Kim^c, W.G. Lynch,
T. Murakami^d, G. Poggi^e, R.T. de Souza^f, M.B. Tsang, and H.M. Xu^g
*National Superconducting Cyclotron Laboratory and Department of Physics and Astronomy,
Michigan State University, East Lansing, Michigan 48824, USA*

K. Kwiatkowski, V.E. Viola, and S. Yennello^h
*Department of Chemistry and Indiana University Cyclotron Facility,
Indiana University, Bloomington, Indiana 47405, USA*

Abstract:

Relative populations of particle unstable states in ^{10}B were measured for the normal kinematics reactions $^{14}\text{N} + ^{27}\text{Al}$ and $^{14}\text{N} + ^{197}\text{Au}$ at $E/A = 75$ MeV, the nearly symmetric reaction $^{129}\text{Xe} + ^{122}\text{Sn}$ at $E/A = 31$ MeV, and the inverse kinematics reaction $^{129}\text{Xe} + ^{27}\text{Al}$ at $E/A = 31$ MeV. In all cases, the relative populations are incompatible with statistical distributions. For the ^{129}Xe -induced reactions, equilibration appears more complete than for the ^{14}N -induced reactions.

PACS number(s): 25.70.Mn, 25.70.Gh

preequilibrium components, while those for the ^{129}Xe -induced reactions are dominated by near-equilibrium decays of rapidly moving heavy projectile and/or fusion residues.

For the calculation of the two-fragment detection efficiency [1], we interpolated the yields for the ^{14}N induced reactions with a simple three-source parametrization, Eq. 1 of ref. [5]; the yields for the ^{129}Xe -induced reactions were interpolated with a two-source parametrization assuming a smooth distribution of Coulomb barriers, Eq. 2 of ref. [5]. The quality of these interpolations is shown by the solid curves in Fig. 1. Most detectors did not allow a clean separation of boron isotopes, but a number of telescopes had sufficient E -resolution to allow determination of the relative yields of B and ^{10}B . In our efficiency calculations, we assumed the angular and kinetic energy distributions of particle stable ^{10}B nuclei and particle unstable $^{10}\text{B}^*$ parent nuclei to be the same as those for isotopically unresolved boron nuclei.

Two-particle correlation functions for $^6\text{Li} + \alpha$ and $^9\text{Be} + p$ are presented in Figs. 2 and 3, respectively, for ^{14}N -induced (upper panels) and ^{129}Xe -induced (lower panels) reactions. The correlation functions were constructed by the "singles" technique:

$$1 + R(q) = C \frac{Y_2(q)}{Y_1(p_1)Y_1(p_2)}. \quad (1)$$

Here, Y_1 and Y_2 denote the single- and two-particle inclusive yields, p_1 and p_2 are the measured momenta of particles 1 and 2, q is the momentum of relative motion, and C is a normalization constant chosen such that $R(q) \rightarrow 0$ for large values of q . The correlation functions show clear peaks due to single states or groups of states resulting from the decays $^{10}\text{B}^* \rightarrow ^6\text{Li} + \alpha$ and $^9\text{Be} + p$. The locations and spins of the relevant states (see Ref. [12] and references therein) are indicated in the panels for the $^{129}\text{Xe} + ^{122}\text{Sn}$ reaction.

In order to extract the populations of particle-unstable states in ^{10}B , the coincidence yield was assumed to be given by $Y_2(q) = Y_c(q) + Y_{\text{back}}(q)$, where $Y_c(q)$ denotes the yield from decays of particle unstable ^{10}B nuclei and $Y_{\text{back}}(q)$ denotes the background yield resulting from coincident emissions of particles 1 and 2 which are not attributed to decays of $^{10}\text{B}^*$ nuclei. The background yield is conveniently expressed [1] in terms of the background correlation function

$$Y_{\text{back}}(q) = [1 + R_{\text{back}}(q)]Y_1. \quad (2)$$

In our analysis, we extracted the coincidence yield for the two extreme assumptions about the background correlation function indicated by the dashed curves in Figs. 2 and 3.

The decay coincidence yield is related to the decay excitation energy spectrum, $\left. \frac{dn(E^*)}{dE^*} \right|_c$, of particle unstable ^{10}B nuclei via the relation

$$Y_c(q) = \int dE^* \left\{ \varepsilon(E^*, q) \left. \frac{dn(E^*)}{dE^*} \right|_c \right\}, \quad (3)$$

distributions (taking particle stable states into account) are plotted as dashed lines with the temperatures indicated in Fig. 4.

For all projectile-target combinations, the population probabilities are inconsistent with thermal distributions, the group of states at $E_\lambda = 6.0$ MeV being more strongly populated than the lower lying group at $E_\lambda = 5.2$ MeV. This observation corroborates previous findings [11-13] of the anomalous role played by the group of states at $E_\lambda = 6.0$ MeV. The distributions for ^{129}Xe -induced reactions reflect a higher degree of equilibration than the distributions for ^{14}N -induced reactions (for which preequilibrium contributions are large at forward angles). Evidence for enhanced equilibration in central, as compared to peripheral $^{36}\text{Ar} + ^{197}\text{Au}$ collisions at $E/A = 35$ MeV had been reported in ref. [13]. It is hence conceivable, that even higher degrees of equilibration could be attained when near-central collisions are selected for the Xe-induced reactions. Experimental corroboration (or disproof) of this assumption would be important as it could provide important clues with regard to the applicability of statistical concepts in heavy-ion-induced fragmentation reactions.

Some deviation from a purely exponential dependence of the population probability can be attributed to sequential feeding from higher lying particle-unbound states. Previous investigations [11-13] have shown, however, that these perturbations cannot explain the inverted population of states around $E_\lambda \approx 6$ MeV. The persistently enhanced population of the group of states at $E_\lambda \approx 6$ MeV for very different reactions suggests that this anomaly may be of a more general origin and independent of details of the reaction dynamics. For example, it is conceivable that the levels in ^{10}B are populated at a stage of the reaction where perturbations by the surrounding hot nuclear matter affect the ordering of levels which evolve into the asymptotic states. Unfortunately such perturbations cannot yet be computed. It is also conceivable that feeding of the group at $E_\lambda \approx 6$ MeV could be governed by branching ratios that differ significantly from those assumed in the Hauser-Feshbach model [12]. Alternatively, the spectroscopic information for ^{10}B may not be complete and there may be an additional unresolved state in the group of levels at $E_\lambda = 6.0$ MeV [17]. In fact, calculations by Warburton et al. [17] predicted a 3^+ state in ^{10}B around an excitation energy of 6 MeV. If such an unresolved state existed and if it were populated according to its statistical weight, it would lead to a decreased population probability for the group at $E_\lambda \approx 6.0$ MeV. The open points in Fig. 4 show how such a state could modify the extracted value of n_λ . We should caution, however, that the existence of this 3^+ state is highly uncertain since, to our knowledge, it has never been confirmed experimentally.

In conclusion, we extracted relative populations of states of particle unstable ^{10}B nuclei in normal kinematics for ^{14}N -induced reactions for ^{27}Al and ^{197}Au targets and compared them to those measured for the inverse kinematics $^{129}\text{Xe} + ^{27}\text{Al}$ reaction and the nearly symmetric $^{129}\text{Xe} + ^{122}\text{Sn}$ reaction. The highest degree of equilibration was observed for the $^{129}\text{Xe} + ^{122}\text{Sn}$ reaction. In all

References

- ^a Present address: Nuclear Science Division, Lawrence Berkeley Laboratory, Berkeley, CA 94720, USA
- ^b Present address: Instituto de Fisica, Universidade de São Paulo, C. Postal 20516, CEP 01498, São Paulo, Brazil.
- ^c Present address: National Lab. for High Energy Physics (KEK), Department of Physics, 1-1 Oho, Tsukuba, Ibaraki 305, Japan.
- ^d Present address: Department of Physics, Kyoto University, Kyoto 606, Japan.
- ^e Present address: Dipartimento di Fisica dell'Universita and INFN, Largo Enrico Fermi 2, 50125 Firenze, Italy.
- ^f Present address: Department of Chemistry, Indiana University Cyclotron Facility, Indiana University, Bloomington, Indiana 47405, USA
- ^g Present address: Cyclotron Institute, Texas A&M University, College Station, Texas 77843, USA
1. J. Pochodzalla et al., Phys. Rev. **C35**, 1695 (1987).
 2. Z. Chen et al., Phys. Rev. **C36**, 2297 (1987).
 3. H.M. Xu et al., Phys. Rev. **C40**, 186 (1989).
 4. G.J. Kunde et al., Phys. Lett. **B272**, 202 (1991).
 5. C. Schwarz et al., Phys. Rev. **C48**, 676 (1993).
 6. W.A. Friedman, Phys. Rev. Lett. **60**, 2125 (1988).
 7. D.H. Boal et al., Phys. Rev. **C40**, 601 (1989).
 8. H.M. Xu, Phys. Lett. **B299**, 199 (1993).
 9. D. Fox et al., Phys. Rev. **C38**, 146 (1988).
 10. C. Schwarz et al., Phys. Lett. **B279**, 223 (1992).
 11. T.K. Nayak et al., Phys. Rev. Lett. **62**, 1021 (1989).
 12. T.K. Nayak et al., Phys. Rev. **C45**, 132 (1992).
 13. F. Zhu et al., Phys. Lett. **B282**, 299 (1992).
 14. W.G. Gong, PhD Thesis, Michigan State University, 1991.
 15. W.G. Gong et al., Phys. Rev. **C43**, 1804 (1991).
 16. W.G. Gong et al., Nucl. Instr. and Meth. **A286**, 190 (1988).
 17. E.K. Warburton and B.A. Brown, Phys. Rev. **C46**, 923 (1992).

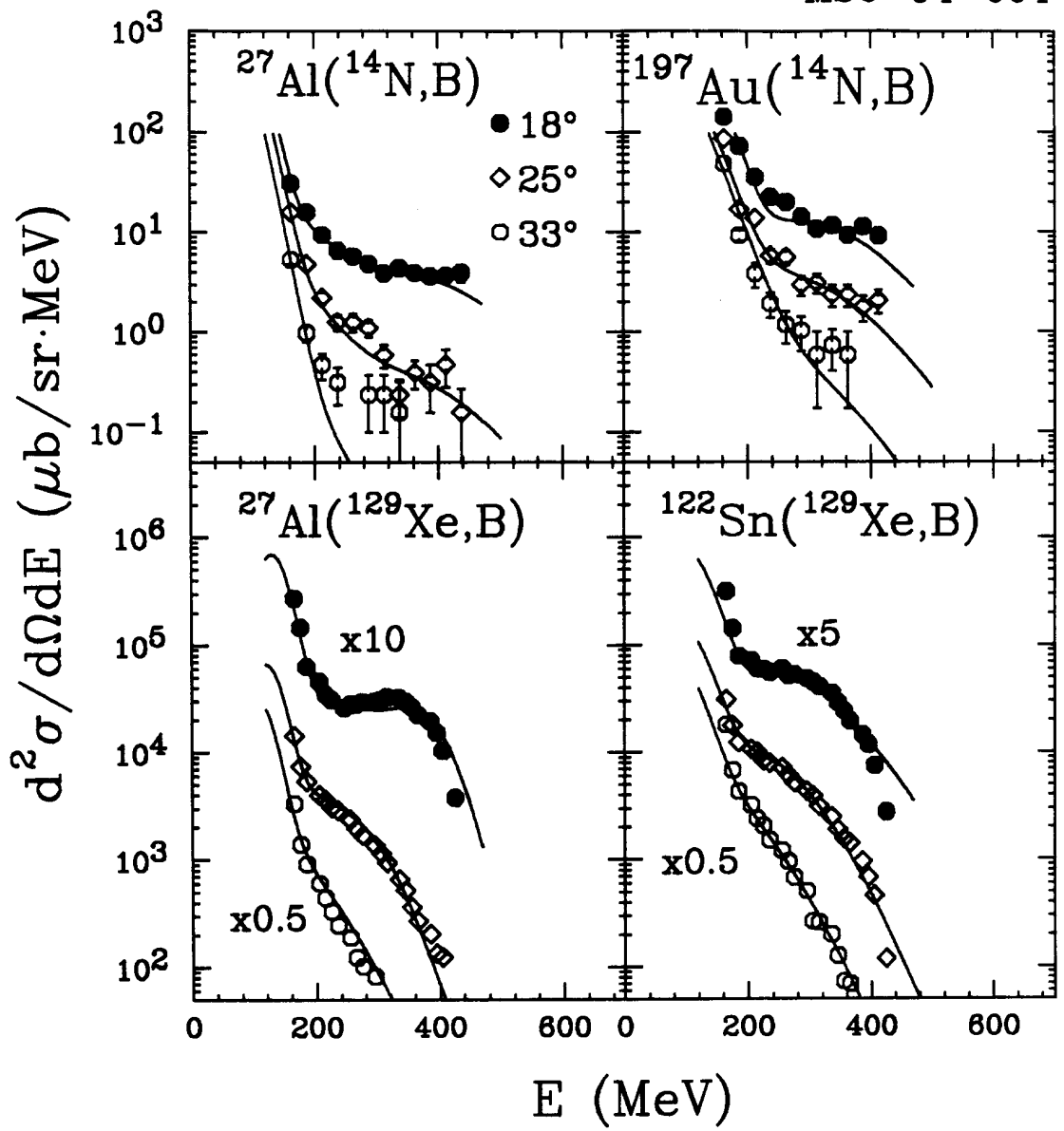


Fig. 1

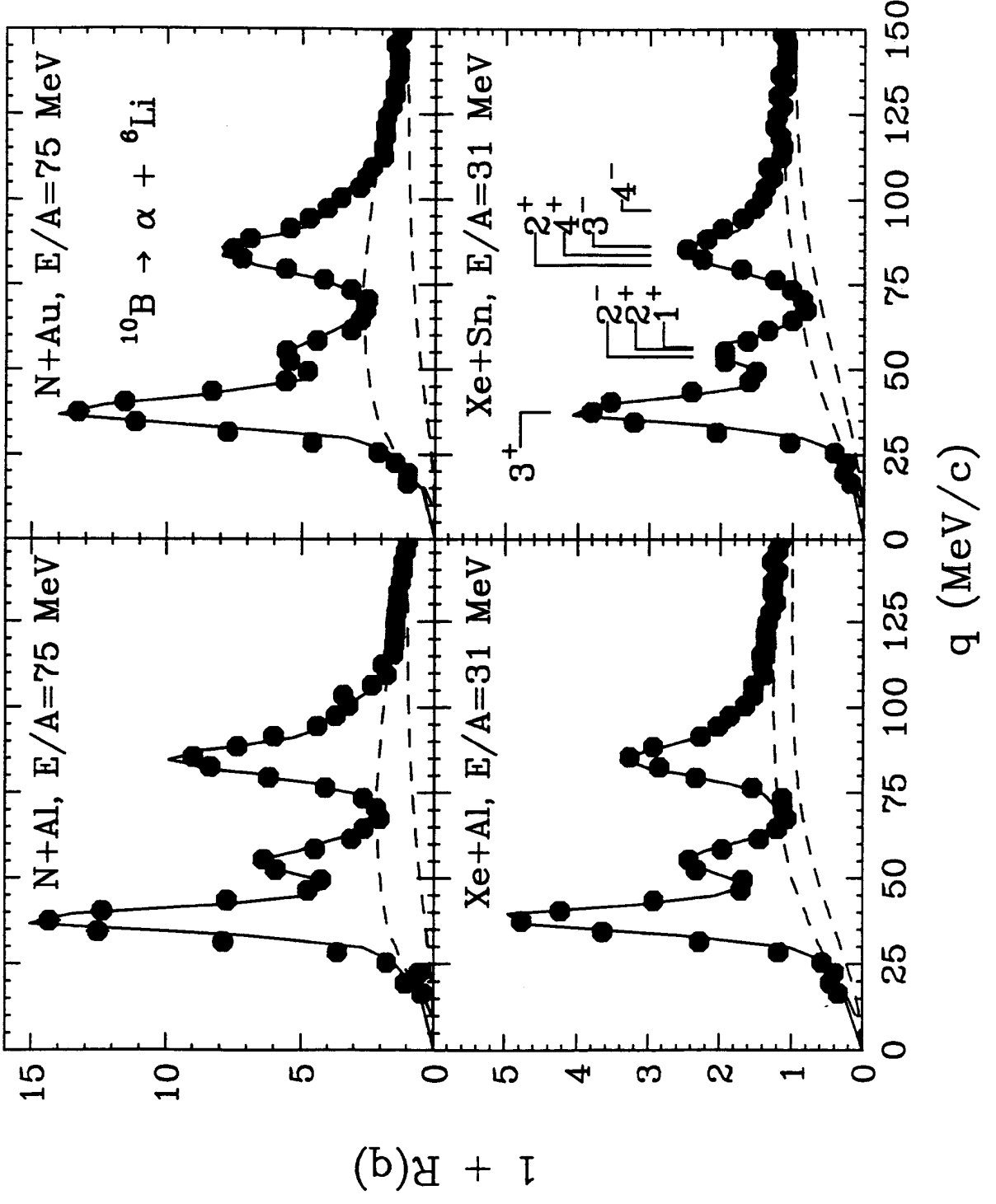


Fig. 2

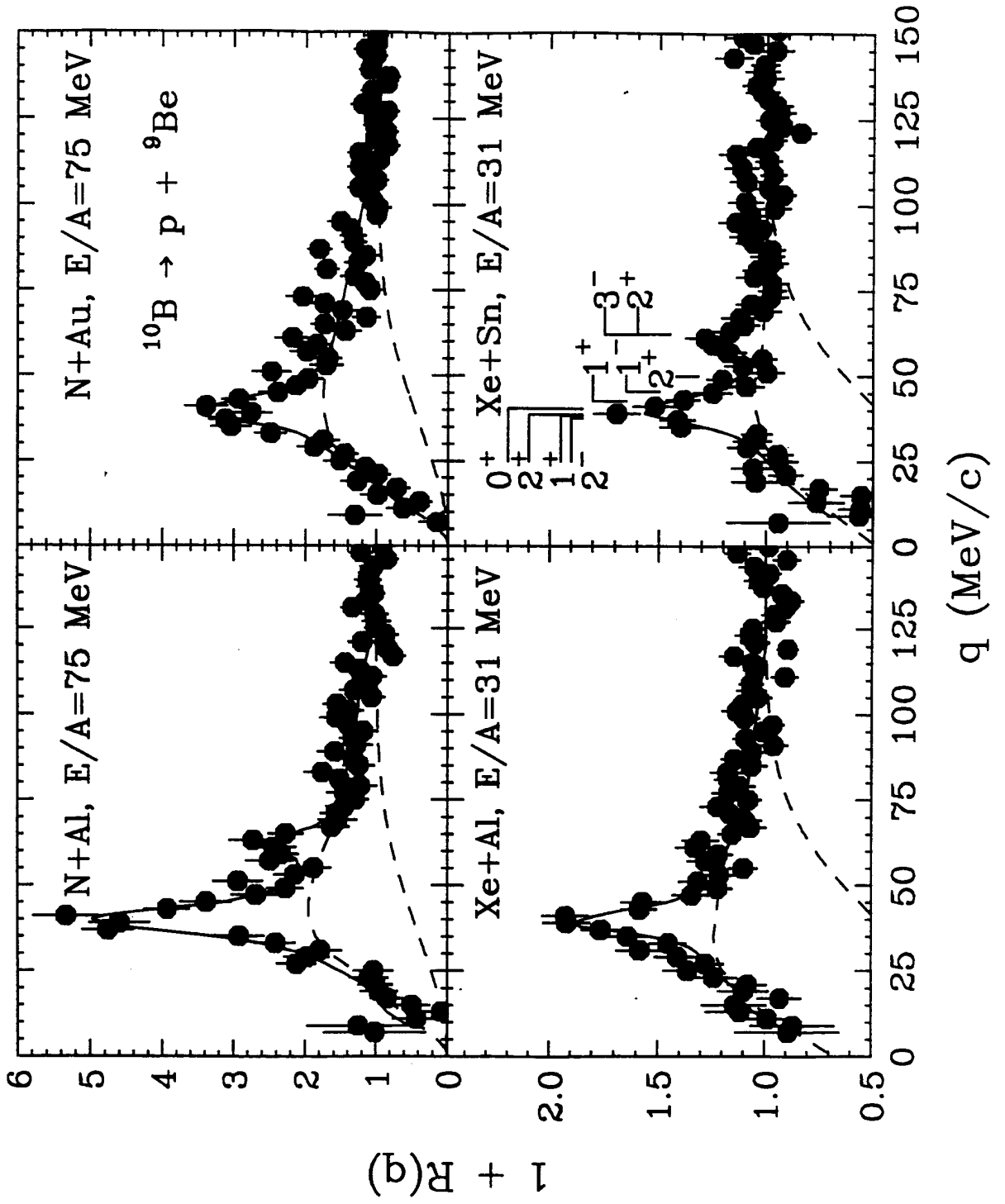


Fig. 3